Corrosion behaviour of post-deposition polished droplets-embedded arc evaporated and droplets-free HIPIMS/DCMS coatings

ARUNACHALAMSUGUMARAN, Arunprabhu <http://orcid.org/0000-0002-5087-4297>, PURANDARE, Yashodhan <http://orcid.org/0000-0002-7544-9027>, EHIASARIAN, Arutiun <http://orcid.org/0000-0001-6080-3946> and HOVSEPIAN, Papken <http://orcid.org/0000-0002-1047-0407>

Published version

ARUNACHALAMSUGUMARAN, Arunprabhu, PURANDARE, Yashodhan, EHIASARIAN, Arutiun and HOVSEPIAN, Papken (2017). Corrosion behaviour of post-deposition polished droplets-embedded arc evaporated and droplets-free HIPIMS/DCMS coatings. Corrosion, 73, 685-693.

Corrosion behaviour of post-deposition polished droplets-embedded arc evaporated and droplets-free HIPIMS/DCMS coatings

Author: 1

Dr. Arunprabhu Arunachalam Sugumaran
National HIPIMS Technology Centre, Sheffield Hallam University, City Campus, Howard Street, Sheffield - S1 1WB, UK.
E-mail: A.Arunachalamsugumaran@shu.ac.uk
Telephone: 0114 225 6322
Fax: 0114 225 3501

Author: 2

Dr. Yashodhan Purandare
National HIPIMS Technology Centre, Sheffield HallamCity Campus, Howard Street, Sheffield - S1 1WB, UK.

Author: 3

Prof. Arutiun Papken Ehiasarian
National HIPIMS Technology Centre, Sheffield Hallam University, City Campus, Howard Street, Sheffield - S1 1WB, UK.

Author: 4

Prof. Papken Ehiasarian Hovsepian
National HIPIMS Technology Centre, Sheffield Hallam University, City Campus, Howard Street, Sheffield - S1 1WB, UK.

Abstract

In this study, the effect of metal rich core of the droplets on the corrosion properties of TiN, CrN and ZrN arc evaporated nitride coatings has been investigated and the corrosion properties of such coatings have been compared with droplet free, highly dense coatings grown by combined high power impulse magnetron sputtering (HIPIMS) and direct current magnetron sputtering (DCMS) technique. An industrial size Hauzer HTC 1000-4 system enabled with HIPIMS technology was used for the deposition of combined HIPIMS/DCMS coatings. The corrosion behaviour of the coatings was studied by potentiodynamic polarisation test (ACM instruments Gill AC potentiostat, -1V to +1V) using 3.5% NaCl solution. Initially, as-deposited arc evaporated coatings with an exposed surface area of 1 cm^2 were subjected to corrosion. Then, the coatings were gently polished to expose the metal rich core of the droplets. Subsequently, fresh un-corroded area of the polished coating was subjected to corrosion with previously corroded area masked. It has been found that mechanical polishing considerably deteriorated the corrosion performance of arc coatings by forming more than one galvanic couple between the two parts (metal rich, nitrogen rich) of the same droplet itself or between the metal rich part of the and the adjoining coating/exposed substrate. It has been further demonstrated that the droplet free highly dense HIPIMS/DCMS coatings exhibited superior corrosion resistance as compared to the arc-evaporated coatings. Raman analysis was used to study the constituents of the corrosion products. Scanning electron microscopy (SEM, planar view) was used to examine the as-deposited and corroded coating surfaces to define morphological differences. Energy dispersive X-ray (EDX) analysis was done to study the composition of the coatings. Cross-section SEM and ball cratering techniques (CSEM calo wear tester) were used to measure the thickness of the coatings.

Keywords: Corrosion resistance, Droplet corrosion, Arc evaporation, HIPIMS, Raman spectroscopy, Corrosion potential.

1. Introduction

Thin film coatings deposited by cathodic arc evaporation and high power impulse magnetron sputtering (HIPIMS) exhibit a highly dense microstructure which is one of the prerequisites for protecting the underlying substrate in a corrosion environment. In both cases, the high degree of ionization [1-4] of the evaporated or sputtered species enhances surface ad-atom mobility which results in growth of dense films.[5, 6] However, thin films deposited by cathodic arc evaporation are known to contain embedded macroparticles (droplets) which are generated during the explosive emission of molten cathode material from the localised volumes heated by arc spots. In reactive cathodic arc evaporation, these droplets undergo incomplete reaction with the reactive gas species during the flight towards the substrate and form a composite coating of rich metal droplets embedded in metal nitride coating matrix. The compositional analysis of such coatings embedded with droplets revealed that the core of the droplets is compositionally metal rich relative to the adjoining compound coating. These embedded droplets then create porosity by shadowing the deposition flux and nucleating large scale growth defects throughout the thickness of the coating. In addition, a voided region is formed beneath each droplet due to atomic shadowing in the region adjacent to the droplets. These defects are believed to contribute in deteriorating the performance of the coatings. Wang et al. proved that the droplets accelerated the substrate corrosion by corroding concurrently with the localised galvanic corrosion of the substrate[7-9]. The detrimental effect of droplets on various coating properties such as adhesion strength, surface roughness and corrosion resistance has been reported elsewhere.[6-8, 10,11] However, according to the authors' knowledge; the literatures discussing the effect of core of the droplets on corrosion resistance of arc evaporated coatings are very less[8].

Generally, in a droplet free PVD coating, galvanic corrosion is initiated between the coating (cathode) and substrate (anode) through the solution present in the defects such as pinholes, pores, micro-cracks and grain boundaries present in the coating.[12,13] However, in arc evaporated coatings, more than one mechanism of galvanic coupling formation is introduced due to the presence of droplets which triggers aggressive localized corrosion.[8]

It is a common practice to polish certain components after deposition to improve surface roughness and appearance of such components. For instance, post-deposition polishing of certain orthopaedic implant components such as femoral head is mainly done to improve its surface roughness. However, in arc evaporated coatings, polishing may expose the pure metal rich core of the droplets which can further deteriorate their corrosion performance. Even if the coatings are not polished after deposition, the droplets are prone to wear out preferentially in tribo-corrosive conditions while articulating another orthopaedic implant component in-vivo which would then expose the metal rich core of the droplets. These cores further complicate the corrosion mechanisms responsible for the corrosion.

During arc evaporation, the emission of the macro particles can be minimized by introduction of magnetic fields in the region near to the cathode. The plasma is steered away from the cathode to the substrate which is not in line of sight, by the combination of magnetic and electric fields generated by the magnetic filters.[14] Various designs of filter have been proposed by several researchers.[15-16] However, it has been reported that the up-scalability of many filters is not easy due to geometry of such filters.[17]

To address this issue, droplet free HIPIIMS technology can be used to deposit such coatings since these coatings exhibited superior corrosion resistance compared to coatings deposited by other PVD techniques.[18,19] In the present work, the effect of metal rich core of the droplets on the corrosion properties of various arc evaporated nitride coatings has been studied and the corrosion properties of such coatings have been compared with droplet free

coatings grown by combined HIPIMS and direct current magnetron sputtering (DCMS) technique. Initially, as-deposited arc evaporated coatings with an exposed surface area of 1 cm^2 were subjected to corrosion. Then, the coatings were gently polished to expose the metal rich core of the droplets. Subsequently, fresh un-corroded area of the polished coating was subjected to corrosion with previously corroded area masked.

2. Experimental details

2.1 Deposition of various nitride coatings using HIPIMS/UBM method

Commercially available arc evaporated TiN, CrN and ZrN coatings were used for this study. In the case of HIPIMS coatings, TiN and ZrN coatings have been deposited on mirror polished stainless steel (SS 304) substrate by a combined HIPIMS/DCMS process using a four cathode industrial size PVD coater (HTC 1000-4) manufactured by Hauzer Techno Coating at Sheffield Hallam University. A detailed description of the PVD coater can be found elsewhere in the literature.[8] Stainless steel substrates were preferred for the deposition since they are a popular choice as substrates for many applications ranging from decorative to biomedical. Four Ti (99.9% pure) and four Zr (99.9% pure) targets were used to deposit the TiN and ZrN coatings respectively. Prior to the deposition of the coating, the substrates were subjected to Ti^{1+} and Zr^{1+} ion bombardment by applying a high bias voltage of - 1000 V to sputter clean the surface and implant Ti ions and Zr ions respectively in order to improve the coating adhesion.[20,21] The coatings were deposited for 4 h in a mixed reactive Ar + N_2 atmosphere at 400 °C. Two of the targets were operated in HIPIMS mode while operating the rest of them in DCMS mode to deposit the combined HIPIMS/DCMS coating. More information on the deposition procedure can be seen in our previous research article. [22]

2.2 Polishing of various nitride coatings deposited by cathodic arc evaporation

Prior to the corrosion test the as-deposited TiN, CrN and ZrN coatings deposited by cathodic arc evaporation were gently polished for few seconds in order to deliberately expose

the core of the droplets present in the coating. For polishing, 1 µm diamond slurry paste on a lapping cloth was used. The surface was examined under scanning electron microscope (SEM) to confirm the effectiveness of the polishing procedure. Following polishing, the samples were cleaned using industrial methylated spirit (mixture of > 94 wt. % of ethanol, 3-4 wt. % of methanol and water) in an ultrasonic bath for 1 minute.

2.3 Characterisation techniques

Potentiodynamic polarisation was used to study the corrosion performance of the coatings. A computer controlled Gill AC potentiostat (ACM instruments) was used to polarise the test specimens. 3.5% NaCl solution was aerated for 20 minutes before immersing the samples to be tested. The test specimens were masked with bees wax to expose a surface area of 1 cm^2. First, the exposed area was cathodically cleaned for 100 s by applying cathodic potential of -1500 mV prior to polarisation. The potentials were recorded with respect to a saturated Ag/AgCl electrode. The sweeping potential was varied from - 1 to +1 V with a scan rate of 1 mVs^{-1} without the reverse cycle. Raman analysis was used to study the constituents of the corrosion products. Raman spectra of as-deposited and corroded samples were recorded by a LabRam HR 800 system (Horiba-Jobin-Yvon) fitted with 532 nm green laser. A 10% transmission filter was utilized to limit the intensity of incident laser beam and to avoid the damage due to irradiation. The samples were exposed to the laser for approximately 5 s for collecting the spectrum. The Raman spectra were acquired in the range between 100 cm^{-1} and 2000 cm^{-1}. SEM (FEI NOVA-NanoSEM 200) coupled with EDX detector was utilised to examine the as-deposited and corroded coating surfaces to define the morphological differences and the composition. Cross-section SEM and ball cratering techniques (CSEM calo wear tester) were used to measure the thickness of the coatings.

3. Results and discussion

3.1 Potentiodynamic polarisation measurements

3.1.1 Pure metal vs as-deposited arc nitride coatings

The potentiodynamic polarisation curves of pure Ti, Cr metals and TiN, CrN metal nitride coatings are shown in Figure 3.1. Table 1 summarizes the corrosion potential (E_{corr}) obtained for such pure metals and nitride coatings. When tested under identical conditions, E_{corr} potentials can demonstrate the (corrosion) tendency of a metal or a coating-substrate system to resist corrosion where more noble E_{corr} values represent higher corrosion resistance. The corrosion current indicates the rate of oxidation and reduction reactions taking place on the specimen surface which is proportional to the corrosion rate. Hence, higher corrosion currents represent enhanced corrosion.[23] The E_{corr} of as-deposited TiN coating (-294 mV) was higher as compared to pure Ti metal (-370 mV). The E_{corr} of as-deposited CrN coating (-182 mV) was much higher as compared to pure Cr metal (-588 mV). The average corrosion current density of pure Cr metal was much higher, 8×10^{-4} A/cm^2 (in the potential range between -588 and +400 mV) as compared to CrN coating 2.1×10^{-4} A/cm^2 (in the potential range between - 182 and +400 mV). A similar behaviour was observed for pure Ti metal and TiN coating in the range between their respective E_{corr} and +300 mV. The high E_{corr} and low corrosion current density (I_{corr}) (Table 1) values of as-deposited TiN and CrN arc nitride coatings demonstrated that such coatings exhibited superior corrosion resistance as compared to their respective pure metal. Hence, for instance, if a nitride coating system is embedded with metal droplets, these droplets being anodic will undergo corrosion by forming a galvanic couple with the adjoining nitride coating (cathode) which remains more noble. It is worth mentioning (Fig. 3.1) that the metal nitride coatings showed excellent corrosion resistance as compared to their respective pure metal form even though the corrosion current of such coatings will also be influenced by the underlying stainless steel substrate if coating defects play a role.

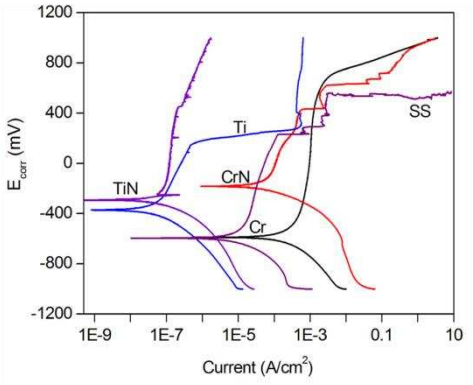

Figure 3.1 Potentiodynamic polarization curves of SS substrate, pure Ti, Cr metal and as-deposited TiN, CrN coatings by arc evaporation technique

Table 1

Thickness and potentiodynamic polarization data of various pure metals and metal nitride coatings deposited on stainless steel substrates

Sample	E_{corr} (mV)	i_{corr} (A/cm^2)	Thickness (µm)
Pure Ti metal	- 370 ± 13	$7.7 \pm 0.71 \times 10^{-5}$ (between -370 and +300 mV)	-
As-deposited TiN (arc) coating	- 294 ± 5	$1.19 \pm 0.06 \times 10^{-7}$ (between -294 and +300 mV)	3.5
Polished TiN (arc) coating	- 277 ± 7	$1.16 \pm 0.05 \times 10^{-7}$ (between -277 and +300 mV)	3.5
As-deposited TiN (HIPIMS) coating	-286 ± 2	$1.01 \pm 0.08 \times 10^{-7}$ (between -286 and +300 mV)	1
Pure Cr metal	- 588 ± 20	$8 \pm 0.79 \times 10^{-4}$ (between -588 and +400 mV)	-
As-deposited CrN (arc) coating	- 182 ± 11	$2.1 \pm 0.23 \times 10^{-4}$ (between -182 and +400 mV)	3
Polished CrN (arc) coating	- 153 ± 5	$7.05 \pm 0.7 \times 10^{-4}$ (between -153 and +400 mV)	3
As-deposited ZrN (arc) coating	- 566 ± 15	$1.69 \pm 0.17 \times 10^{-5}$ (between - 566 and -240 mV)	2.5
Polished ZrN (arc) coating	- 527 ± 9	$3.86 \pm 0.41 \times 10^{-5}$ (between - 527 and -240 mV)	2.5
As-deposited ZrN (HIPIMS) coating	-399 ± 8	$1.36 \pm 0.11 \times 10^{-5}$ (between - 399 and -240 mV)	2

3.1.2 Arc nitride coatings

The gentle polishing procedure mentioned in section 2.2 deliberately exposed the metal rich core of the droplets present in the coatings. Subsequently these polished areas of the coatings were subjected to corrosion tests.

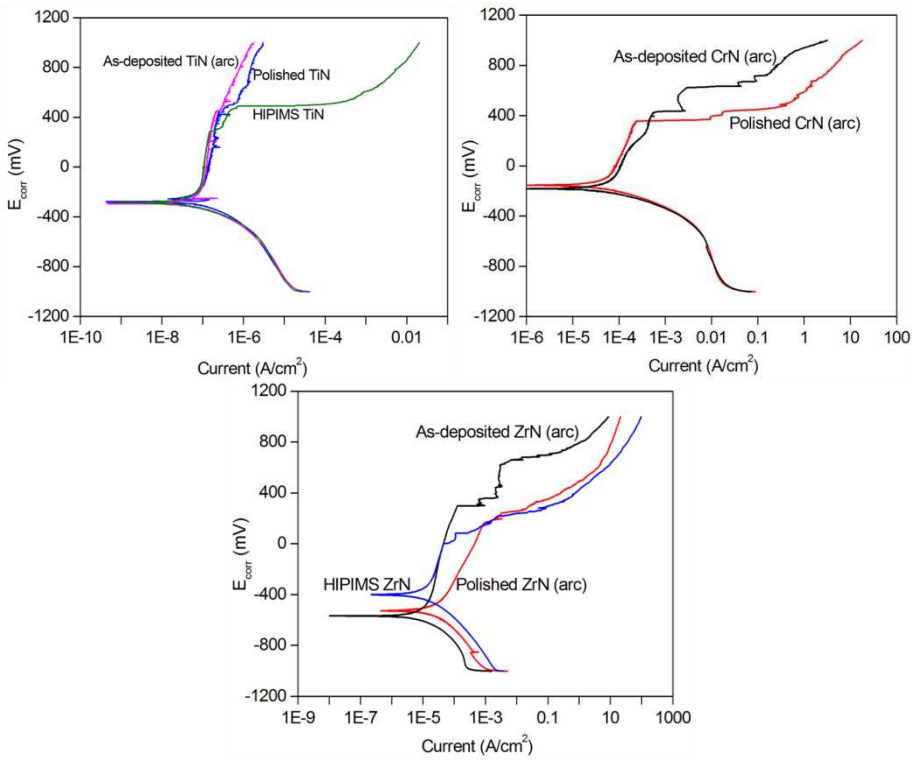

Figure 3.2 Potentiodynamic polarization curves: a) as-deposited, polished arc TiN nitride coatings and combined HIPIMS/DCMS TiN coating, b) as-deposited, polished arc CrN nitride coatings, c) as-deposited, polished arc ZrN nitride coatings and combined HIPIMS/DCMS ZrN coating

The effect of polishing on corrosion current can be clearly seen in Figure 3.2 (a-c). For CrN, the I_{corr} of polished coating (7.05 x 10^{-4} A/cm^{-2}, in the potential range from -153 to +400 mV) was higher than the as-deposited coating (2.10 x 10^{-4} A/cm^{-2}, in the potential range from -182 to +400 mV). In the case of ZrN, the I_{corr} of polished coating was 3.86 x 10^{-5} A/cm^{-2} (in the potential range from -527 to -240 mV) as compared to the as-deposited coating, 1.69 x 10^{-5} A/cm^{-2} (in the potential range from - 566 to -240 mV). The I_{corr} of TiN polished coating was slightly higher, 1.16 x 10^{-7} A/cm^{-2} (in the potential range from -277 to +300 mV) as compared to that of as-deposited, 1.19 x 10^{-7} A/cm^{-2} (in the potential range from -294 to +300 mV) coating. The low corrosion current density of as-deposited coatings implied that such coatings showed better corrosion resistance than the polished coatings. The poor corrosion performance in these potential ranges of the polished coatings can be attributed to the metal rich core of droplets which was exposed by polishing along with the possibility of

removing the droplet defect completely, thereby exposing the substrate. The corrosion mechanism of droplet embedded composite nitride coating is complex and can be explained as follows. The as-deposited (unpolished) droplet which was embedded at the beginning of the deposition may be fully or partially covered with nitride coating and can form more than one galvanic couple between one part of itself as anode and another as cathode since they are compositionally heterogeneous. Also, the whole droplet itself can act as an anode relative to the adjoining coating and trigger localized corrosion of the droplets. However a through thickness droplet can also be cathodic to the substrate.[8] In addition, when these droplets are polished, if intact, the metal rich core of the droplets are completely exposed to electrolyte which further complicates the corrosion mechanism. This metal rich core of the droplets can form more than one galvanic couple with surrounding nitrogen rich area. Thus the metal rich core of the droplets further accelerates the localized corrosion. The voids present beneath the droplets may also deteriorate the corrosion performance by allowing the electrolyte to react with the underlying substrate. Hence, the corrosion mechanisms acting on the coating surface will be comprised of corrosion of the coating, contribution from the exposed substrate as well as galvanic effects between the coating elements.

3.1.3 Arc nitride coatings vs combined HIPIMS/DCMS nitride coatings

The corrosion behaviour of as-deposited and polished coatings deposited by arc evaporation was compared with droplet free HIPIMS/DCMS deposited coatings. Figure 3.2 (a and c) depicts TiN and ZrN coatings deposited by combined HIPIMS/DCMS along with arc deposited coatings. HIPIMS/DCMS deposited ZrN coating exhibited much higher corrosion potential (-399 mV) than the arc counterparts (as-deposited: -566 mV and polished: - 527 mV). The E_{corr} of HIPIMS/DCMS TiN (- 286 mV) coating was slightly higher than the arc deposited coatings (as-deposited: -294 mV and polished: - 277 mV). The higher E_{corr} values of HIPIMS/DCMS coatings indicated the improved corrosion resistance of such

coatings. The i_{corr} of HIPIMS ZrN was low, 1.36 x 10^{-5} A/cm^{-2} (in the potential range from -399 mV to -240 mV) as compared to arc coatings (as-deposited: 1.69 x 10^{-5} A/cm^{-2}, in the potential range from -566 to -240 mV and polished: 3.86 x 10^{-5} A/cm^{-2}, in the potential range from -527 to -240 mV). The i_{corr} of HIPIMS TiN was also lower,1.01 x 10^{-7} A/cm^{-2} (in the potential range from -286 mV to +300 mV) as compared to arc coatings (as-deposited: 1.16 x 10^{-7} A/cm^{-2}, in the potential range from -294 to +300 mV and polished: 1.19 x 10^{-7} A/cm^{-2}, in the potential range from -277 to +300 mV). This excellent corrosion behaviour in these potential ranges is attributed to droplet free highly dense microstructure due to high energy ion bombardment by HIPIMS which eventually enhances the adatom mobility on the surface of the growing film.[6] However, the corrosion current density of these coatings was higher after -240 mV for ZrN and + 300 mV for TiN as compared to their respective arc evaporated coatings. This may be due to thinner HIPIMS coatings used for this study as compared to arc counterparts and the influence of defects (related to contamination from the deposition chamber)[24] present in the coatings. The role of defects (enhanced due to the corrosion) is more evident at higher anodic potentials and can be attributed to the fact that the solution has more time to permeate through the thickness of the coatings to reach underlying substrate. In this study, uniform coatings with various thicknesses have been compared as these samples were part of a bigger study concerning various aspects of PVD processes. Moreover, arc deposited samples were commercially sourced; hence their properties and thicknesses were out of control. Figure 3.3 shows cross section SEM images of highly uniform TiN and ZrN coatings deposited by combined HIPIMS/UBM technique. The thickness of arc deposited ZrN coating was about 2.5 µm whereas it was only 2 µm for HIPIMS ZrN. The arc deposited TiN coating was much thicker (3.5 µm) as compared to HIPIMS/DCMS TiN (1 µm) coating. In summary, the increased E_{corr} values and lower corrosion currents of HIPIMS coatings (in the potential range from -399 to -240 mV for ZrN and from -286 to +300 mV for TiN)

suggested that they provide better corrosion resistance than arc evaporated coatings due to enhanced density of the coatings and the absence of droplets (related defects such as voids beneath droplets).

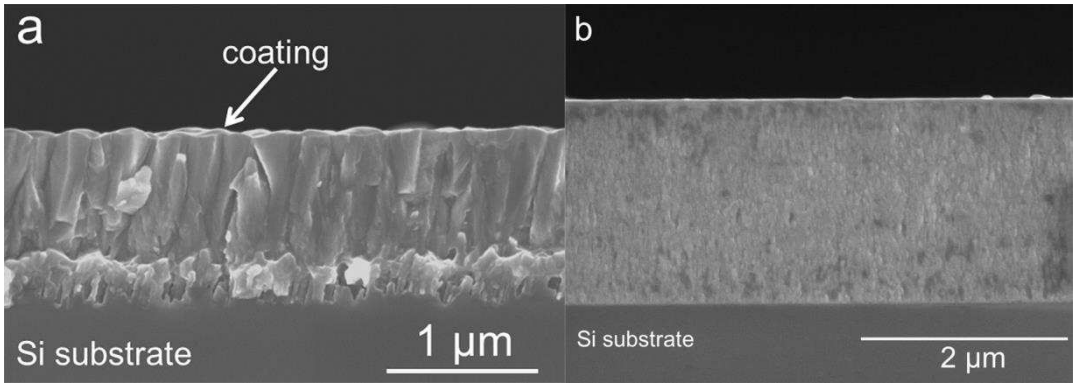

Figure 3.3 Cross section SEM images: a) combined HIPIMS/DCMS TiN coating, b) combined HIPIMS/DCMS ZrN coating

3.2 Plan view SEM analysis

3.2.1 Arc nitride coatings

Figure 3.4 shows the plan view SEM images of various as-deposited, polished and corroded nitride coatings deposited by arc evaporation method. Figure 3.4 (a, d & g) show as-deposited TiN, ZrN and CrN coatings The droplets embedded in all the three coatings can be clearly seen along with the small craters. The craters are believed to have appeared after the ejection of droplets embedded close to the film surface as a result of weak droplet-coating bonding due to the presence of voids beneath droplets.[7]

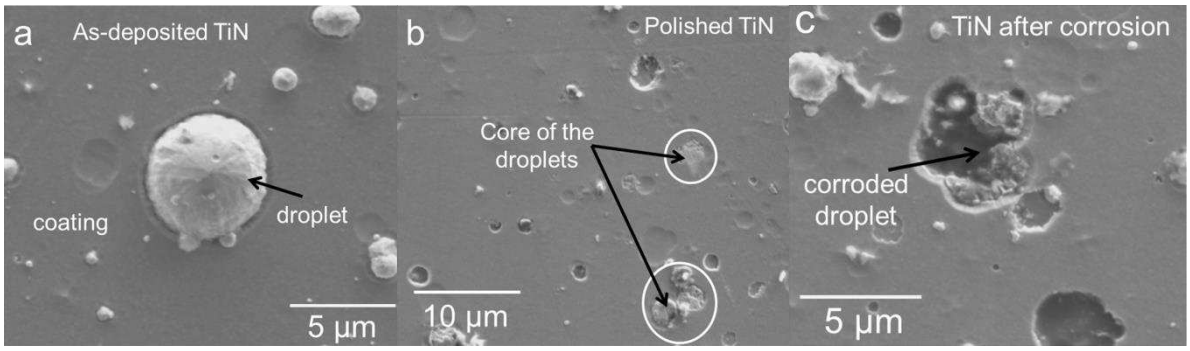

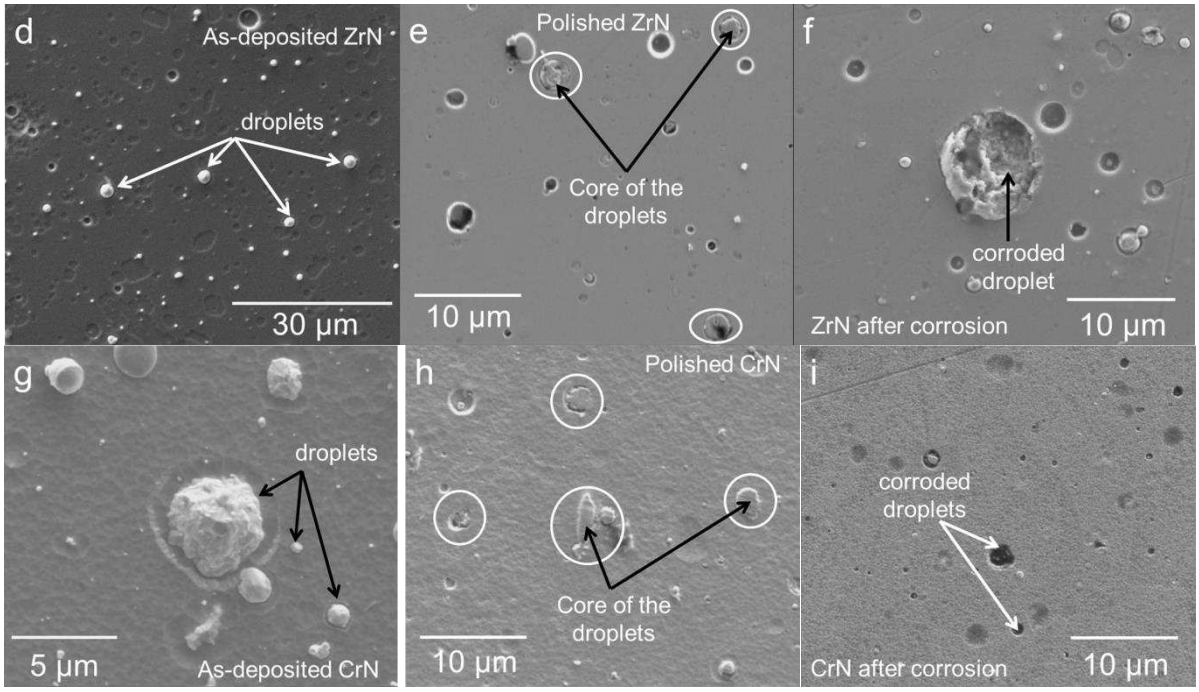

Figure 3.4 Plan view SEM images: a) as-deposited arc TiN coating, b) polished arc TiN coating, c) corroded arc TiN (after polishing) coating, d) as-deposited arc ZrN coating, e) polished arc ZrN coating, f) corroded arc ZrN (after polishing) coating, g) as-deposited arc CrN coating, h) polished arc CrN coating, i) corroded arc CrN (after polishing) coating

Figure 3.4 (b, e, h) show the plan view SEM images of polished TiN, ZrN and CrN coatings deposited by arc evaporation. It can be clearly seen that the droplets were either completely removed or partially ground during the polishing. The remains of partially-ground droplets (circled in white) confirmed that the polishing effectively exposed the core of droplets.

Figure 3.4 (c, f, i) show the plan view SEM images of TiN, ZrN and CrN coatings which were subjected to corrosion after polishing. The corrosion experimental setup was same for all samples and explained in sec 2.3. These SEM images showed that the droplets were mainly affected by the corrosion while the coating was still intact. Some of the droplets are partly dissolved and few are almost completely dissolved due to the droplet corrosion. Interestingly, some the droplets are still completely intact and not affected by the corrosion. Each of the damaged droplets leaves a through-thickness hole or cavity as a consequence of the corrosion. This hole or cavity can be identified by different colour contrasts of such hole

or cavity, the undamaged droplets and the neighbouring coating. These findings can be correlated with the potentiodynamic polarisation measurements.

3.2.2 **Combined HIPIMS/DCMS nitride coating**

Figure 3.5 shows plan view SEM images of as-deposited and corroded TiN coating deposited by combined HIPIMS/DCMS technique. It can be clearly seen that the as-deposited coating was free of droplets. After corrosion analysis, the corroded surface showed tiny pinholes as compared to arc deposited coatings which exhibited such defects in a large-scale and size.

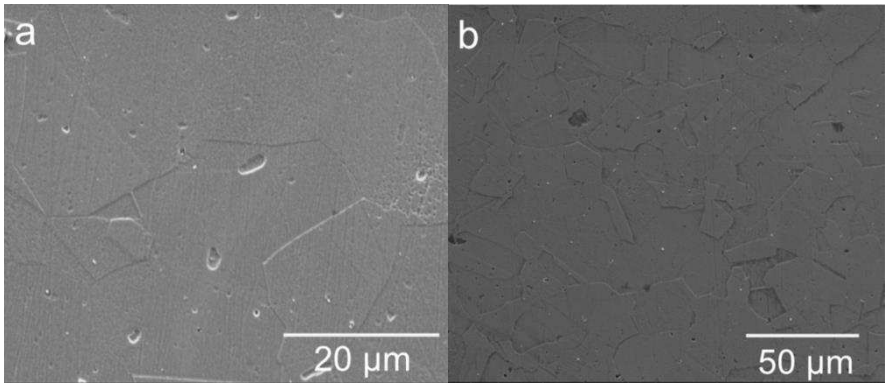

Figure 3.5 Plan view SEM images of combined HIPIMS/DCMS coating: a) as-deposited TiN coating, b) corroded TiN coating

3.3 Energy dispersive X - ray (EDAX) and Raman analysis

EDAX and Raman analysis have been done to demonstrate the effect of droplet corrosion in TiN, CrN and ZrN coatings deposited by arc evaporation. Table 3.2 lists the composition of such as-deposited, polished and corroded coatings.

Table 2 Composition of various as-deposited, polished metal nitride coatings and droplets embedded on polished metal nitride coatings

Sample	Elements present (%)						
	Ti	Cr	Zr	N	Fe	Mn	Ni
As-deposited TiN (arc) coating	38			62			
Polished droplet on as-deposited TiN (arc) coating	86			14			
Corroded droplet on TiN (arc) coating	30	10			51	1	8
As-deposited CrN (arc) coating		42		58			
Polished droplet on as-deposited CrN (arc) coating		64		36			

Corroded droplet on CrN (arc) coating	54			41	1	4
As-deposited ZrN (arc) coating		58	42			
Polished droplet on as-deposited ZrN (arc) coating		100				
Corroded droplet on ZrN (arc) coating	14	10		63	2	11

EDAX analysis revealed that as-deposited TiN and CrN coatings were over-stoichiometric whereas as-deposited ZrN was sub- stoichiometric. The EDX of polished droplets in all three coatings confirmed that the core of such droplets was rich in metal [Table 2]. These results are in agreement with the findings of Ljungcrantz et al.[7] Therefore, polishing has effectively exposed the metal rich core of the droplets. It is worth mentioning that the composition of few unpolished droplets was almost similar to the composition of coating [not shown in the Table 2] as they were covered with metal nitride coating after embedding on the growing coating surface. The EDX analysis of corroded droplets in all three coatings showed the presence of corrosion products such as Fe, Mn, Ni and Cr due to substrate corrosion as they are being the major constituents of stainless steel. It has been reported that oxides, hydroxides, oxy hydroxides, nitrates, nitrides, sulphates, chlorides and oxy chlorides of Fe, Cr and Ni could be formed due to substrate (SS 304) corrosion.[25]

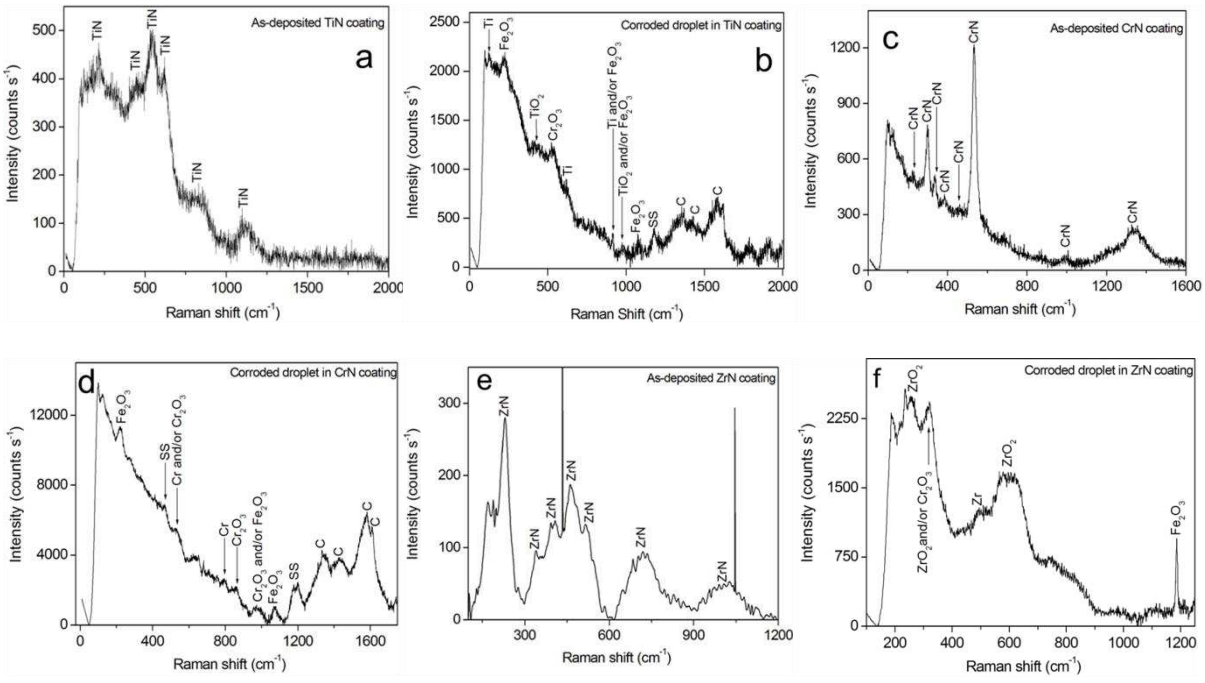

Figure 3.6 Raman analysis a) as-deposited arc TiN coating, b) corroded droplet in arc TiN coating, c) as-deposited arc CrN coating, d) corroded droplet in arc CrN coating, e) as-deposited arc ZrN coating, f) corroded droplet in arc ZrN coating

Figure 3.6 shows Raman spectra of various arc deposited nitride coatings and corroded droplets present in the coating surface. Table 3 lists Raman data and assignment of Raman peaks for stainless steel, metal nitride coatings and corrosion products. Characteristic phonon bands were observed for as-deposited TiN, CrN and ZrN coatings. Generally, metal nitride coatings are likely to form a passive layer along with compounds such as oxynitrides when subjected to corrosion. In addition, compounds include oxides of Fe, Cr and Ni could be formed due to stainless steel (substrate) corrosion.[25] Raman analysis of uncoated corroded stainless steel confirmed that oxides of such compounds were formed due to substrate (SS 304) corrosion. Raman analysis of corroded droplets revealed the formation of oxides such as TiO_2, Cr_2O_3, ZrO_2 and Fe_2O_3 due to corrosion. These findings further confirmed that the droplets were susceptible to corrosion. In addition, Raman peaks for pure metal elements such as Ti, Cr and Zr were also observed from the corroded droplets and it could be due to the fact that the core of the droplets is rich in metal. It can be concluded that metal rich core of the droplets triggers the corrosion.

Table 3 Raman data

Sample	Peak assignment Raman shift (cm^{-1})
Corroded SS substrate	224 - Fe_2O_3[26] 270, 348, 386, 470 529 - Cr_2O_3[27,28] 653 - Fe_2O_3[26] 856 - CrO_2 + Cr_2O_3[27] 978 - Fe_2O_3[26] 1083 1338,1432 and 1579 - amorphous carbon from atmospheric carbon and corrosion[29]

As-deposited TiN (arc) coating	218, 453, 545, 613, 833 and 1101 - TiN[30]
Corroded droplet in TiN (arc) coating	122 220 - Fe_2O_3[26] 420 - TiO_2 526 - Cr_2O_3[27,28] 817 - Ti and/or Fe_2O_3[26] 974 - TiO_2 and/or Fe_2O_3[26] 1078 - Fe_2O_3[26] 1178 - corrosion product from SS 1353,1424 and 1582 - amorphous carbon from atmospheric carbon and substrate corrosion[29]
As-deposited CrN (arc) coating	225, 300, 337, 385, 455, 536, 996, 1344 - CrN[28,31]
Corroded droplet in CrN (arc) coating	219 - Fe_2O_3[26] 335 - CrN and/or Cr_2O_3[28] 467 - corrosion product from SS 525 - Cr_2O_3[27,28] 637 797 - Cr 859 - Cr_2O_3 967 - Cr_2O_3 and/or Fe_2O_3[26] 1068 - Fe_2O_3[26] 1198 - corrosion product from SS 1335,1427, 1580 and 1609 - amorphous carbon from atmospheric carbon and corrosion[29]
As-deposited ZrN (arc) coating	169, 230, 276, 340, 408,463, 516, 720,1027 - ZrN[30]
Corroded droplet in ZrN (arc) coating	255 - ZrO_2[32] 320 - ZrO_2 and/or Cr_2O_3[28,32] 491 - Zr 596 - ZrO_2[32] 1256 - Fe_2O_3[26]

4 Conclusions

The corrosion mechanism of metal rich core of droplets embedded in arc evaporated coatings is illustrated. Potentiodynamic polarisation measurements revealed that as-deposited (arc) coatings exhibited better corrosion resistance as compared to their polished counterparts as the mechanical polishing exposed metal rich core of the droplets to the electrolyte which triggered localized corrosion. The implantation of droplets can happen anytime during the coating deposition process. Hence, though not visible from the surface, it can be present in the coating. It will be challenging to show the contribution of the droplet macroparticles only

to the overall corrosion current since it is very difficult to isolate them or to pinpoint the exact moment of complete dissolution of the droplets during the corrosion test due to their size variations and placement limitations. Nevertheless, in this study, potentiodynamic polarisation results have been reproducible in which the corrosion current densities of as-deposited coatings have been lower as compared to the polished coatings. Therefore, if the components coated with arc coatings are polished after deposition to improve its surface roughness and appearance, then the corrosion properties of such coatings are compromised. SEM, EDAX and Raman analyses also confirmed that the metal rich core of the droplets were susceptible to corrosion. To overcome this drawback, droplet free highly dense HIPIMS coatings can be used for such applications as they exhibited enhanced corrosion resistance compared to the arc evaporated coatings.

References

1. I.G. Brown, "Vacuum arc ion sources," Rev. Sci. Instrum. 65 (1994): p. 3061.
2. A. Anders, G.Y. Yushkov, "Ion flux from vacuum arc cathode spots in the absence and presence of a magnetic field," J. Appl. Phys. 91 (2002): p.4824.
3. R. Franz, C. Clavero, R. Bolat, R. Mendelsberg, A. Anders, "Observation of multiple charge states and high ion energies in high-power impulse magnetron sputtering (HiPIMS) and burst HiPIMS using a LaB6 target," Plasma Sources Sci. Technol. 23 (2014): p. 035001.
4. J. Andersson, A.P. Ehiasarian, A. Anders, "Observation of Ti^{4+} ions in a high power impulse magnetron sputtering plasma," Appl. Phys. Lett. 93 (2008): p. 071504.
5. D.M. Sanders, A. Anders, "Review of cathodic arc deposition technology at the start of the new millennium," Surf. Coat. Tech. 133 - 134 (2000): p. 7890.

6. A.P. Ehiasarian, A. Vetushka, Y. A. Gonzalvo, G. Safran, L. Szekely, "Influence of high power impulse magnetron sputtering plasma ionization on the microstructure of TiN thin films," Journal of applied physics 109, (2011): p. 104314.
7. H. Ljungcrantz, L. Hultman, J.-E. Sundgren, G. Håkansson, L. Karlsson, "Microstructural investigation of droplets in arc-evaporated TiN films," Surf. Coat. Tech. 63, 1–2 (1994): p.123.
8. H.W. Wang, M.M. Stack, S.B. Lyon, P. Hovsepian, W.-D, Münz, "The corrosion behaviour of macroparticle defects in arc bond-sputtered CrN/NbN superlattice coatings," Surf. Coat. Tech. 126, 2–3 (2000): p. 279.
9. I. Petrov, P. Losbichler, D. Bergstrom, J.E. Greene, W.-D. Münz, T. Hurkmans, T. Trinh, "Ion-assisted growth of $Ti_{1-x}Al_xN/Ti_{1-y}Nb_yN$ multilayers by combined cathodic-arc/magnetron-sputter deposition," Thin solid films, 302, (1–2) (1997): p. 179.
10. C. Liu, A. Leyland, S. Lyon, A. Matthews, "Electrochemical impedance spectroscopy of PVD-TiN coatings on mild steel and AISI316 substrates," Surf. Coat. Tech. 76-77, (1995): p. 615.
11. M. Lakatos-Varanyi, D. Hanzel, "Cyclic voltammetry measurements of different single-, bi- and multilayer TiN and single layer CrN coatings on low-carbon-steel substrates," Corros. Sci. 41, (1999): p.1585.
12. W.-D, Münz, T. Hurkmans, G. Keiren, T. Trinh, "Comparison of TiAlN coatings grown by unbalanced magnetron and arc bond sputtering techniques," J. Vac. Sci. Technol. A 11, (1993); p. 2583.
13. D.B. Lewis, S.J. Creasey, C. Wustefeld, A.P. Ehiasarian, P.Eh. Hovsepian, "The role of the growth defects on the corrosion resistance of CrN/NbN superlattice coatings deposited at low temperatures," Thin Solid Films 503, (2006): p. 143.

14. ANDERS, André Cathodic arcs. [online]. Last accessed 08/07/2013 at: http://escholarship.ucop.edu/uc/item/5km1m68m.
15. S. Ramalingam, Q.B. Cai, K. Kyunghoon, "Controlled vacuum arc material deposition, method and apparatus," US 4673477A, 1987.
16. A. ANDERS, "Approaches to rid cathodic arc plasmas of macro- and nanoparticles: A review," Surf. Coat. Tech. 120–121, (1999): p.319.
17. U. Helmersson, M. Lattemann, J. Bohlmark, A.P. Ehiasarian, J.T. Gudmundsson, "Ionized physical vapor deposition (IPVD): A review of technology and applications," Thin solid films 513 (1–2), (2006): p.1.
18. Y. Purandare, A. Ehiasarian, A. Santana, P. Hovsepian, "ZrN coatings deposited by high power impulse magnetron sputtering and cathodic arc techniques," J. Vac. Sci. Technol. A 32, (2014): p.031507.
19. Y. P. Purandare, A. P. Ehiasarian, P. Eh. Hovsepian, "Deposition of nanoscale multilayer CrN/NbN physical vapor deposition coatings by high power impulse magnetron sputtering," J. Vac. Sci. Technol. A 26, (2008): p.288.
20. A.P. Ehiasarian, P. Eh. Hovsepian, W.-D. Münz, "A Combined Process Comprising Magnetic Field-Assisted, High-Power, Pulsed Cathode Sputtering and an Unbalanced Magnetron," EP 1 260 603 A2, DE 10124749, 2001.
21. A.P. Ehiasarian, J. G. Wen and I. Petrov, "Interface microstructure engineering by high power impulse magnetron sputtering for the enhancement of adhesion," J. Appl. Phys.101, (2007): p. 054301.
22. P.Eh. Hovsepian, A.A. Sugumaran, Y. Purandare, D.A.L. Loch, A.P. Ehiasarian, "Effect of the degree of high power impulse magnetron sputtering utilisation on the structure and properties of TiN films," Thin solid films 562, (2014): p. 132.
23. L. Yang, Techniques for corrosion monitoring (Cambridge, UK: Woodhead

publishing limited, 2008): p.54.

24. P. Eh. Hovsepian, A.P. Ehiasarian, Y.P. Purandare, B. Biswas, F.J. Pérez, M.I. Lasanta, M.T. de Miguel, A. Illana, M. Juez-Lorenzo, R. Muelas, A. Agüero, "Performance of HIPIMS deposited CrN/NbN nanostructured coatings exposed to 650 °C in pure steam environment," Mater. Chem. Phys. (in press): DOI:10.1016/j.matchemphys.2016.05.017.
25. S. Ramya, T. Anita, H. Shaikh, R.K. Dayal, "Laser Raman microscopic studies of passive films formed on type 316LN stainless steels during pitting in chloride solution," Corros. Sci. 52, 6 (2010): p. 2114.
26. RRUFF - Online data base of Raman spectroscopy
27. A. Öztürk, K.V. Ezirmik, K. Kazmanlı, M. Ürgen, O.L. Eryılmaz, A. Erdemir, "Comparative tribological behaviours of TiN-,CrN- and MoN-Cu nanocomposite coatings," Tribol. Int. 41, 1 (2008): p. 49.
28. A Barata, L Cunha, C Moura, "Characterisation of chromium nitride films produced by PVD techniques," Thin Solid Films 398-399, (2001): p. 501.
29. Radhika Ramadoss, N. Kumar S. Dash, D. Arivuoli, A.K. Tyagi, "Wear mechanism of CrN/NbN superlattice coating sliding against various counterbodies," Int. Journal of Refractory Metals and Hard Materials 41, 2013: p. 547.
30. C.P. Constable, J. Yarwood, W.-D. Münz, "Raman microscopic studies of PVD hard coatings," Surf. Coat. Tech. 116-119, **(**1999): p. 155.
31. X. Y. Zhang and D. Gall, "CrN electronic structure and vibrational modes: An optical analysis, Phys. Rev. B 82, (2010): p. 045116.
32. P. Barberis, T. Merle-Mrjean, P. Quintard, "On Raman spectroscopy of zirconium oxide films," J. Nucl. Mater. 246, 1997: p. 232.